A MATHEMATICAL SIMULATION OF ACCIDENTAL EMISSIONS AS A METHOD OF IMPROVING OPTICAL MONITORING OF ATMOSPHERIC POLLUTION

K.Ya Kondrat'ev, V.I. Khvorost'yanov, O.P. Kotova, and N.I. Cherkasova

Central Aerological Observatory, Dolgoprudnyi
Received June 10, 1991

A routine mathematical model of a contaminating specie spreading in the boundary atmospheric layer after accidental emission is developed for organizing an optimal network of optical monitoring of industrial emissions into the atmosphere, based on a solution of system of equations involving: 1) equations of motion and turbulence energy budget for calculating the turbulence and wind modes; 2) equations of temperature and moisture transfer, accounting for their diurnal time—behavior; 3) equation of turbulent diffusion, describing transfer of a weightless passive contaminant for various scenarios of an accident; and, 4) the heat equation in soil and equation of heat balance of a surface. Numerical calculations have been performed and general features of the evolution of a contaminant cloud at different values of the geostrophic wind G and the degree of roughness r_0 are investigated. The results are compared with those calculated according to the Gaussian model of a diffusive flow. It is shown that the developed numerical model enables one to describe, better than the Gaussian method, the fields of a contaminant spreading during a nonstationary emission after an accident for assessment of the influence of industrial plants on environment and the development of the system of protection measures. These results and a PC compatible model can be used for optimization of the network of optical sensing, their density and location for various scenarios of accidents.

Introduction. Rates of anthropogenic pollution of the atmosphere through ordinary and accidental emissions have sharply increased during recent years. Optical monitoring is one of the ways to control the air pollution and determine the maximum permissible emission (MPE).

It is expedient to equip the industrial objects which can potentially contaminate the atmosphere with toxic and explosive materials (especially during accidents) with a network of optical sensors capable of measuring pollutants concentrations in air. Such an optical system should, of course, be optimized, i.e., 1) have a sufficient number of optimally located sensors for collecting data on the whole field of concentrations, especially during an accident emission and 2) not to be too cumbersome and expensive.

Mathematical modeling is one of the ways of improving the optical monitoring of pollution.[1] An advantage of modeling is the possibility of obtaining information about the spatio—temporal evolution of the increased contamination zones and about their horizontal and vertical scales. This enables one to estimate the necessary number of optical sensors and density of their network for various scenarios of an accidental emission.

A whole hierarchy of diffusion models has been currently made up with different levels of complexity, operativeness and completenessof taking physical processes into account.[2–6]

There exist models of two kinds: the local based on the Gaussian—type models (more simple but incapable of taking a whole number of meteorological processes into account) and the mesoscale covering the scales of several hundred meters up to 200 km, which are more complete physically

and can be performed on modern computers in a routine mode.

The model presented in this paper belongs to the second kind. The contamination spreading in the boundary atmospheric layer after an accident or a sanctioned emission is modeled taking into account the following combination of the atmospheric processes: the advective and turbulent transfer with a detailed calculation of the three—dimensional fields of turbulence and wind, heat and humidity exchange between air and the underlying surface, diurnal temperature behavior, and radiation transfer in the atmosphere.

Formulation of the system of equations. Let us direct the x axis along the geostrophic wind velocity G. The system of equations for the dynamics of the atmospheric boundary layer (ABL) includes equations of motion, the horizontal components of the wind velocity u and v, the discontinuity equation for the vertical wind velocity w, the balance equation for the turbulent energy b, the likelihood and dimensionality ratios, and the hypothesis of closure for the mixing path l (Refs. 4—6):

$$\frac{\partial u}{\partial t} + \mathrm{div}\, u\mathbf{U} = \tilde{\Delta} u + f_c\left(v - V_g\right),$$

$$\tilde{\Delta} = \frac{\partial}{\partial x}\, k_x \frac{\partial}{\partial x} + \frac{\partial}{\partial y}\, k_y \frac{\partial}{\partial y} + \frac{\partial}{\partial z}\, k_z \frac{\partial}{\partial z}, \tag{1}$$

$$\frac{\partial v}{\partial t} + \mathrm{div}\, v\mathbf{U} = \tilde{\Delta} v + f_c\left(u - U_g\right), \tag{2}$$

$$-\frac{\partial u}{\partial x} = \frac{\partial v}{\partial y} + \frac{\partial w}{\partial z} , \tag{3}$$

$$\frac{\partial b}{\partial t} + \text{div } b\mathbf{U} = k_z \left[\left(\frac{\partial u}{\partial z}\right)^2 + \left(\frac{\partial w}{\partial z}\right)^2 + \right.$$

$$\left. + \left(\frac{\partial v}{\partial z}\right)^2 - \frac{q}{T}\frac{\partial \Theta}{\partial z} \right] - \varepsilon - \alpha_B \tilde{\Delta} b , \tag{4}$$

$$k = l\sqrt{b}, \; \varepsilon = c_1 b^{3/2} l ,$$

$$l = -\kappa \; l^{1/4} \sqrt{\frac{b}{l}} \left[\left(1 + \frac{k}{U_0}\right)\frac{\partial}{\partial z}\sqrt{\frac{b}{l}} \right]^{-1} . \tag{5}$$

Here $f_c = 2\omega \cdot \sin\varphi$ is the Coriolis parameter (ω is the angular rotation frequency of earth, φ is the latitude), k is the coefficient of turbulence, ε is the rate of energy dissipation, $\kappa = 0.4$ is the von Karman constant, $\alpha_B = 0.73$ and $c_1 = 0.046$ are the empiric coefficients, Θ is the potential temperature, V_g and U_g are the components of the geostrophic wind, and T is the temperature.

This system describes the turbulence and wind variations due to the advective and convective transfer and turbulent diffusion. The terms in the right–hand side of Eq. (4) describe, respectively, the generation of b due to the wind shear and the effect of buoyancy forces, and the dissipation and diffusion of b. The effect of temperature stratification on the turbulence and wind is taken into account wich respect of the term containing $\frac{\partial \Theta}{\partial z}$ and by choosing the coefficients in form (5).

The fields of temperature Θ and humidity in the model can be calculated by solving the transfer equations for q and Θ accounting for the diurnal behavior of temperature

$$\frac{\partial \Theta}{\partial t} + u \frac{\partial \Theta}{\partial x} + v \frac{\partial \Theta}{\partial y} + w \frac{\partial \Theta}{\partial z} = \tilde{\Delta}\Theta , \tag{6}$$

$$\frac{\partial q}{\partial t} + u \frac{\partial q}{\partial x} + v \frac{\partial q}{\partial y} + w \frac{\partial q}{\partial z} = \tilde{\Delta}q. \tag{7}$$

To account for heat and moisture exchange between the atmosphere and the underlying surface as well as for diurnal temperature behavior on the surface we have solved the heat and heat balance equations for surface

$$\frac{\partial T_s}{\partial t} = k_s \frac{\partial^2 T_s}{\partial z^2} , \; \rho_a c_p k \frac{\partial \Theta}{\partial z} - L\rho_a k \frac{\partial q}{\partial z} - c_s \rho_s k_s \frac{\partial T_s}{\partial z} = 0 . \tag{8}$$

Here T_s, ρ_s, c_s, and k_s are the temperature, density, heat capacity, and thermal conductivity of the soil and ρ_a is the density of the atmosphere

The transfer of the weightless passive specie is described by the equation of turbulent diffusion:

$$\frac{\partial c}{\partial t} + u \frac{\partial c}{\partial x} + v \frac{\partial c}{\partial y} + w \frac{\partial c}{\partial z} = \tilde{\Delta}c + \alpha(t), \tag{9}$$

where c is the average value of the specie concentration.

Based on experimental and theoretical studies we conclude that the emission scenario includes three types of situations: 1) spilling of a liquified gas and its evaporation from the surface of the spill; 2) rupture of a pressurized reservoir or a pipe–line with succeeding effluent; and, 3) leakage under overpressure. The fact that the emission may have several stages with different parameters of the source power is taken into account.[9–11]

Evolutions of the accidental emission for the constant and variable source power are considered below.

Initial and boundary conditions for the ABL are determined by the specific type of the modeled process.[11] In the present case, since the horizontal size of the area under study is small (3 km along the x axis, and 1.5 km along the y axis), the initial fields of temperature and humidity are taken to be horizontally uniform:

$T(x, y, z) = T_0 - \gamma z q(x, y, z) = q_{si}[1 -(1 - q_{ro})\exp(z/AD)]$,

i.e., temperature decreases linearly as a function of an altitude with the gradient γ, and the relative humidity has the value q_{ro} near the surface and its undersaturation decreases e–fold at the height AD.

The quasistationary state of the boundary layer in the flow over the horizontally uniform surface is taken as the initial condition for calculating the dynamics of the turbulence and wind; $\mathbf{U}$, b, k, and l profiles are calculated by solving Eqs. (1)–(5) at constant T_0 and γ and their derivatives with respect to x are equal to zero. A parameter of roughness z_0 is varied in calculations that enables one to take into account the type of underlying surface. Boundary conditions for T and q at $x = x_1 = 0$ are determined from solutions of Eqs. (6) and (7) without advective terms, and for $x = x_2$ as

$$\frac{\partial T}{\partial x} = \frac{\partial q}{\partial x} = 0 .$$

On the underlying surface (the level of roughness is equal to z_0) the boundary conditions for the temperature are the heat balance equation and the heat equation for the soil (Eqs. (9) and (10)), for humidity it is the condition of matching the molecular and turbulent fluxes of moisture[5,11]

$$k\rho_a \frac{\partial q}{\partial z} = a_{ef} \frac{v_b}{4}(q - q_{si}),$$

where a_{eff} is the effective coefficient of condensation and v_b is the velocity of water vapor molecules. In addition, $u = v = w = k \frac{\partial f}{\partial z} = 0$. On the upper boundary of the ABL

$$u = U_g, \; v = U_g ,$$

$$k = \frac{\partial f}{\partial z} = k \frac{\partial q}{\partial z} = 0, \frac{\partial T}{\partial z} = -\gamma.$$

The boundary conditions for a pollutant are similar to those described in Refs. 2 and 3: on the ground and the left boundary they are the conditions of reflection and on the right boundary they are the conditions of penetration.

The calculations were performed on an ES–1052 computer. The calculational grid cell was $\Delta x = 50$ m, $\Delta z = 5$ m, and $\Delta y = 50$ m along the x, y, and z exes, respectively. The numbers of nodes are $N_x = 61$, $N_y = 31$, and $N_z = 31$. Time of computations for a typical variant was 20 min (time step $\Delta t = 150$ sec that corresponded to 30 sec of computer time).

Evolution of the contaminating specie cloud after an accidental emission. The calculations presented below used the following set of parameters, which we call the basic set: $T_0 = 15°C$, $f_c = 10^{-4}$ sec^{-1}, the heat capacity, the thermal conductivity, and the density of soil are equal to $C_s = 0.25$ cal/(g·°C), $k_s = 4.6^{-3}$ cm^2/sec, and $\rho_s = 2$ g/cm^3, respectively, the size of the calculational area along the x, y, and z axes are 3 km, 1.5 km, and 150 m, respectively.

The rupture of a tank on the ground was modeled, for this purpose, the emission having the contaminating specie flux density $P(t)$ with the cross section S (S was equal to 20 cm^2 in all calculations) was set at the point x. Then the effluent rate was derived from formulas

$$Q = P \cdot S, \ \dot{V} = \mathbf{U} \cdot \delta_z \cdot \delta_y, \ c_{max}(t) = \frac{Q}{\dot{V}} = \frac{P(t) \cdot S}{\mathbf{U} \cdot \delta_z \cdot \delta_y}, \qquad (10)$$

where V is the volume of the specie spreading per unit time and C_{max} is the greatest value of the specie concentration at the point of emission. The contaminating flux is taken to be constant, i.e., continuous emission of substance through the reservoir rupture is modeled. The geostrophic wind velocity G and the value of the roughness z_0 are varied. The table presents the summary of the main variants of numerical experiments.

Figure 1 shows the calculated profiles of the turbulent diffusion coefficient k_z (Fig. 1a) and wind component u (Fig. 1b) for different values of the geostrophic wind and roughness of underlying surface.

An increase of G from 2 to 5 m/s results in the wind velocity increase at every point of space, e.g., at the height of a windwane it rises from 0.7—0.9 m/sec for $G = 2$ (Fig. 1b, variant 1) and to 1.9—2.3 m/sec for $G = 5$ (Fig. 1b, variant 3). But an increase of roughness z_0 a retardation of the flux occurs and, consequently, the value of wind is lower for the same values of the geostrophic wind. For example, for $G = 2$ m/sec, $z_0 = 1$ (variant 1) and $z_0 = 100$ (variant 2) the values of wind at the height of a windwane are equal to 0.7—0.9 and 0.3—0.5 m/sec, respectively.

TABLE I. The summary of the variants of numerical experiments

Variants	Geostrophic wind velocity G, m/sec	Value of roughness z_0, cm	Wind velocity G_u, m/sec at the height 5 m/10 m	Rate of emission from the source Q, g/sec
1	2	1	0.7/0.9	10^3
2	2	100	0.3/0.5	10^3
3	5	1	1.9/2.3	10^3
4	5	100	0.6/1.0	10^3
5	—	—	2/2	10^3
6	—	—	5/5	10^3

Note. Variants 1—4 are the detailed calculations of the fields of wind and turbulence, variants 5—6 are for a Gaussian model.

The value of the coefficient of turbulent diffusion k_z grows with G and z_0 (Fig. 1a). For an enhanced roughness the greatest value of k_z shifts upward along the vertical axis.
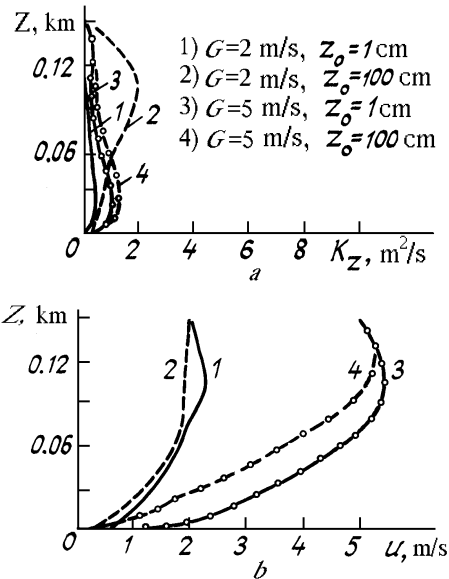

FIG. 1. Vertical profiles of the fields of turbulent diffusion coefficients k_z (a) and wind component u (b) for variants 1—4.

The contaminating specie evolution for a ground—based continuous source is calculated with an account of the above—indicated fields of wind and turbulence. Figure 2 shows the calculated vertical profiles of the fields of the specie concentration for $G = 2$ and 5 m/sec, $z_0 = 1$ for different moments of time (asterisk denotes the source of emission). Isolines of the substance concentration look like plumes with its axis directed along the geostrophic wind, i.e., along x axis, already 10 min after the starting of the emission (Fig. 2a). The plume length along the x axis grows with increase of the effluent time (Fig. 2b), the zone of the contaminating specie spreading increases, or more correct, it is broadened in all directions. For example, for variant 1 (the level of roughness is $z_0 = 1$ cm and $G = 2$ m/sec) the zone of the spreading along the x axis is equal to 1.5 km 10 min after the starting of the emission, and along the z axis it is equal to 60 m, while along the y axis it is equal to 300 m (Fig. 2a). Then 20 min after these distances are 2.5 km, 90 m, and 300 m, respectively, (Fig. 2b). In addition, the separation of the plume from the ground occurs with distance from the emission point and time of calculation) this is caused, first, by the growth of the turbulence coefficient k_z in the layer 0—30 m along the vertical direction (Fig. 1a) and, second, due to the growth of the wind velocity with height.

Since the emission source is continuous the largest value of the contaminating specie concentration attains at the emission point and its temporal growth (storage) occurs ($c_{max} = 0.046$ g/cm^3 for $t = 10$ min and $c_{max} = 0.08$ g/cm^3 for $t = 20$ min). The growth of the geostrophic wind G up to 5 m and, as a consequence, the growth of the wind component u and the decrease of k_z leads to faster spreading of the contaminating specie upwards along the flux (Fig. 2, dashed curves). For example, after 20 min (Fig. 2b) the zone of contaminating specie concentration $\log c = 7.5$ (here and in the figures the concentration is represented by its logarithm) reaches the value of 1.1 km along the x axis and 35 m — along the z axis for $G = 2$ m/sec and for $G = 5$ m/sec — 2.5 km and

70 m, respectively. But, because of the k_z decrease the end of the plume is pressed down to the ground, and no essential separation occurs, as in the case of $G = 2$ m/sec with time of effluence.
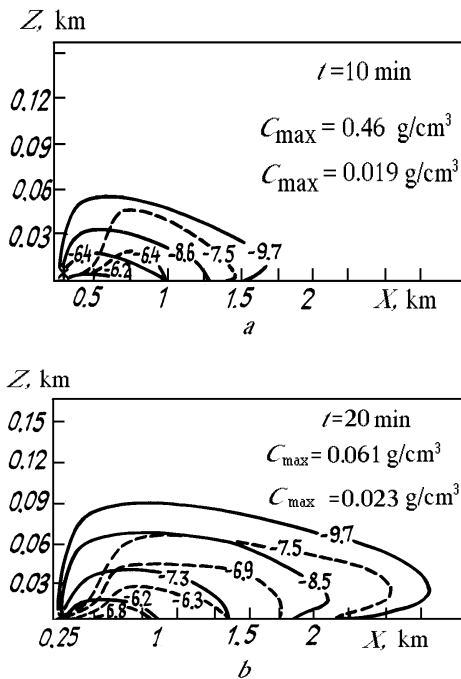

FIG. 2. Vertical profile of the fields of the contaminating specie concentration in the ZOX–plane for $t = 10$ min (a) and $t = 20$ min (b), variants 1 (solid curves) and 3 (dashed curves); are isolines of concentration in log c units.

Fast spreading of the contaminating specie leads to a decrease of its accumulation at a certain point.

Thus, the value of the maximum contaminating specie concentration reduces to $c_{max} = 0.019$ g/cm³ for $t = 10$ min and to $c_{max} = 0.028$ g/cm³ for $t = 20$ min. It follows from comparison of the results that

$$\frac{c_1(t)}{c_2(t)} = \frac{c_2}{c_1},\tag{11}$$

where $c_1 = c_{max}$ for the variant of calculation with $G = G_1$ and $c_2 = c_{max}$ for $G = G_2$.

Calculations for $z_0 = 1$ cm and $z_0 = 100$ cm were performed for studying the effect of roughness z_c on the evolution of the contaminating cloud.

Figure 3 shows the calculated vertical and horizontal profiles of the fields of the contaminating specie concentration for variants 1–2 40 min after the beginning of the emission. $G = 2$ m/sec and $z_0 = 1$ cm (variant 1, solid curve), $z_0 = 100$ cm (dashed curve). As can be seen from Fig. 3, isolines of the concentration show that the effluent takes the shape of a plume, but the horizontal length of the isolines for the same value of c decreases (e.g., the length of isolines for $\log c = -7.5$ along the x axis is equal to 2.25 km for variant 1 and 1.75 km for variant 2), and the vertical length increases ($z = 0.5$ and $z = 0.7$ km, respectively) with increase of roughness for the same values of G. This can evidently be explained by greater value of the coefficient of the turbulent diffusion and retardation of

the flux. The retardation of the flux also leads to accumulation of the specie at a certain point, in particular, the maximum value of the contaminating specie concentration at the emission point is $c_{max} = 0.0076$ g/cm³ for $z = 1$ cm and $c_{max} = 0.11$ g/cm³ for $z = 100$ cm. Increase of the coefficient of turbulence also leads to a faster separation of the plume tail.
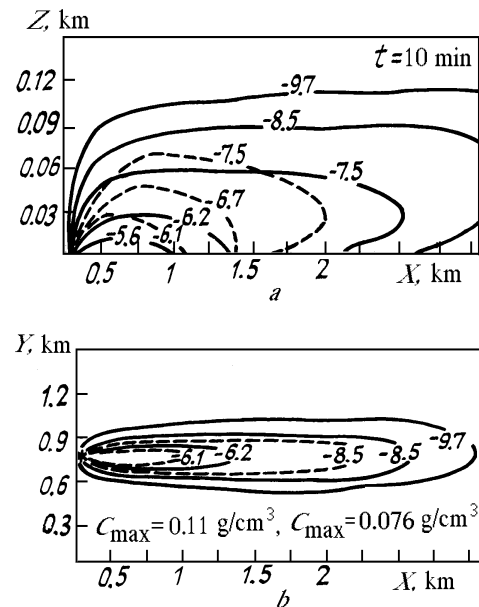

FIG. 3. Vertical cross section in the ZOX plane (a) and the horizontal one in the XOY plane (b) of the fields of the contaminating specie concentration for $t = 40$ min, solid curves are for variant 1 and dashed curves are for variant 2; isolines of concentrations are given in log c units.

The value of roughness is determined by the landscape type. Thus, in particular, the value $z_0 = 1$ cm corresponds to a plain and $z_0 = 100$ cm is characteristic of a forest or an urban area, and, as is shown above, the roughness essentially effects on the contaminating specie cloud spreading, that should necessarily be taken into account for correct description of real situations of accidental and ordinary emissions.

The presented–above numerical experiments determine the contaminating specie spreading from a continuous constant source, $P(t) = $ const, that corresponds, e.g., to the emission from a pipe–line leakage, leak of volatile materials through small cracks in buildings containing pollutants.

An approach dealing with an emission of explosive materials, splitting of substance with its further evaporation into the atmosphere can be modeled by assigning the source, whose power is described as a decreasing function of time $P = M_0\delta(t - t_0) + P_0\exp(-t/t_0)$, where t_0 is the parameter characterizing the scale of such a decrease for the density of the contaminating specie flux.

This situation can be conditionally divided into two simultaneous processes: 1) "instant point–source" or formed in a short period of time puff of the contaminating specie moving from the source along the wind direction, the amount of substance in the puff is $\sim M_0 S\Delta t$; 2) steady source with the density P_0. Figure 4 presents the horizontal fields of a contaminating specie spreading at different time for the source of a given concentration.
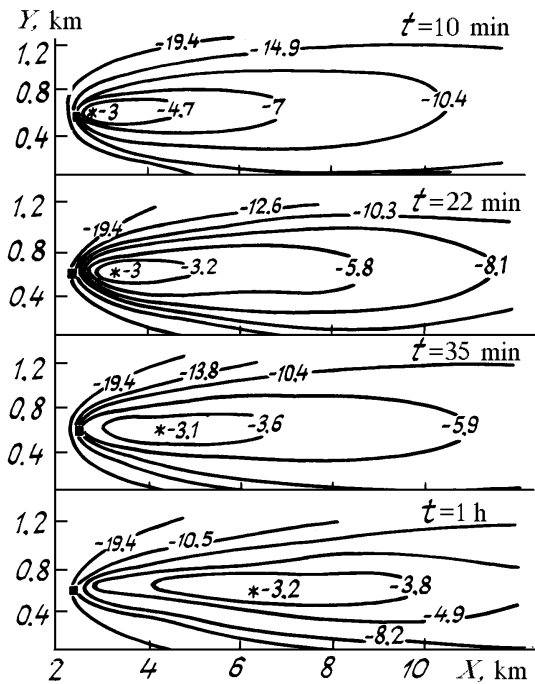
FIG. 4. Horizontal cross section of the fields of the contaminating specie concentration in the XOY plane for a source of the type $P = M_0\delta(t - t_0) + P_0\exp(-t/t_0)$.

Calculations show that isolines of the substance concentration also take the shape of the plumes with its axis directed along the geostrophic wind, i.e., they are qualitatively correspond to the picture of contaminating specie spreading from a steady source. But, the maximum value of the substance concentration (log $c_{max1} = -3.1$), the "puff—center" is reached not at the source point, but at a point shifted along the wind direction at a distance depending on time. This maximum value is determined by the puff formed in the initial 10–15 min of the emission and its position moves as the puff moves, the puff itself being broadened with time.

In fact, the horizontal distribution of the contaminating specie concentration is bimodal. The second maximum with the lower value of concentration is located at the point of emission source, but the concentration near the source decreases with time (e.g., log $c_{max2} = -4.7$ for $t = 10$ min and log $c_{max2} = -5.9$ for $t = 30$ min). This situation is caused by the two contradicting processes: 1) the growth of the contaminating specie concentration near the source due to the accumulation of substance coming from the steady source and 2) by the fall of concentration due to the turbulent and wind transfer and relative contributions coming from these processes depend both on the dynamic characteristics of the atmosphere and on the emission parameters P_0 and t_0.

Therefore, the described—above numerical experiments enable one to study the effect of the type of emission source, wind velocity, and roughness of the underlying surface on the formation of the fields of contamination in the case of an accidental emission. The calculated fields of the contaminating specie concentration make it possible to evaluate the specie (of a fixed initial concentration) spreading area at any time after the emission outburst provided that meteorological conditions are known and to determine the zones in which the maximum and permissible

concentration is surpassed, as well as to estimate the concentration excess.

Comparison with the Gaussian methods. Calculations according to the Paskvill method for a steady—point source[7,10] were performed to compare the developed numerical model with the Gaussian diffusion model of a flow. An equation for the contaminating specie concentration under conditions of a negligible diffusion along the x axis in comparison with wind transfer along the same direction is

$$c = \left(2\pi\sigma_y\sigma_z\,\overline{u}\right)^{-1}Q'\exp\left(-\frac{y^2}{2\sigma_y}\right) \times$$

$$\times \left\{\exp\left[-\frac{(z-h)^2}{2\sigma_z^2}\right] + \exp\left[-\frac{(z+h)^2}{2\sigma_z^2}\right]\right\}, \tag{12}$$

where h is the distance from the ground to an elevated source, Q' is the power of a steady source, σ_y and σ_z are the variances of the distribution of concentration along the y and z axes, determined from the series of curves for various classes of the atmospheric stability derived by Paskvill from experiments.[10]
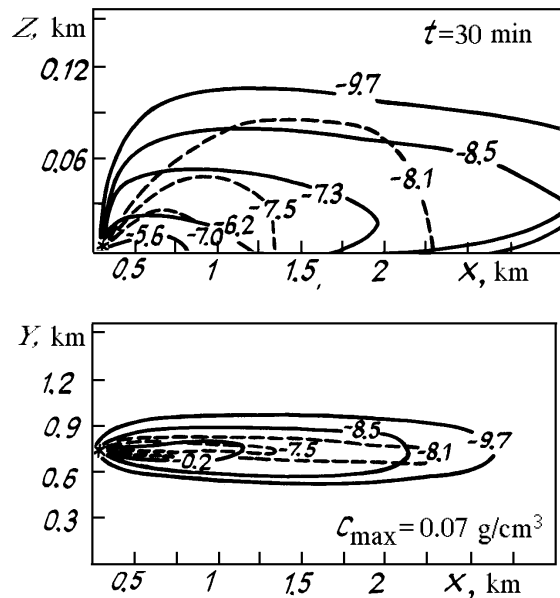

FIG. 5. Vertical cross section in the ZOX plane (a) and the horizontal one in the XOY plane (b) of the fields of a contaminating specie concentration calculated according to the method with detailed calculation of the fields of wind and turbulence for variant 1 (solid curves) and by the Gaussian method for variant 5 (dashed curves).

Figure 5 shows the vertical and horizontal cross sections of the contaminating specie concentration calculated by the Gaussian method (dashed curves) and by the above—described model (solid curves) for the value $G = 2$ m/sec. As it follows from Fig. 5, the results of calculations differ from each other, though both models yield the plume like a shape of the fields of concentration formed due to the specie spreading. But, since a constant wind velocity is an intrinsic feature of the Gaussian model, it cannot describe the separation of the plume tail from the ground because it is, first of all, connected with the profile of the wind velocity.

The stationary Gaussian model cannot describe correctly the evolution of the contaminating cloud giving the largest distortions of an actual process just for the beginning of the emission (accident). This makes it impossible to take into account the effect of the roughness of surface, which can be essential, as the above calculations have shown. With increasing wind velocity an "extension" of the contamination zone occurs simultaneously with decrease of concentration.

Thus, for a correct evaluation of the fields of the weightless admixture concentration, a thorough calculation of the fields of turbulence and wind is needed, which is impossible for a wide interval of parameters within the frameworks of the Gaussian models, but can be performed using the numerical model presented in this paper.

Conclusion. Numerical experiments enable one to evaluate the parameters of the zone of a contaminating specie spreading at a given moment after the emission outburst provided that the meteorological situation is known. The results were compared with the results of the Gaussian method for a diffuse flow[12] for various values of wind and the comparison revealed that the Gaussian model is less correct for describing the dependence of the fields of concentration on the wind velocity. Calculations of horizontal length of the zone where the contaminating specie concentration exceeds the MPC (and the value of the excess) are extremely important not only for estimation of the effect of industrial plants on the environment and ecological situation after ordinary routine emissions, but also for predicting the consequences of accidental emissions. It is especially important for optimizing the optical monitoring of the atmospheric pollution, in particular, for obtaining the routine data on the entire field of a contaminating specie, based on which we can choose the necessary number of optical sensors and density of their network.

This model is quite an operative one and can be applied to control of a given object using a personal computer combined with a system of optical sensors.

REFERENCES

1. M.E. Berlyand, *Modern Problems of the Atmospheric Diffusion and Atmospheric Pollution* (Gidrometeoizdat, Leningrad, 1975), 448 pp.
2. A.S. Monin and A.M. Yaglom, *Statistical Hydromechanics*, Pt. 1 (Nauka, Moscow, 1965); Pt. 2 (Nauka, Moscow, 1967).
3. G.I. Marchuk, *Mathematical Simulation in the Problem of Environmental Protection* (Nauka, Novosibirsk, 1985), 289 pp.
4. V.V. Penenko and A.E. Aloyan, *Models and Methods in the Problems of Environmental Protection* (Nauka, Novosibirsk, 1985), 256 pp.
5. *Meteorology and Nuclear Energy* (Mir, Moscow, 1968).
6. G.I. Marchuk, K.Ya Kondrat'ev, V.V. Kozoderov, and V.I. Khvorost'yanov, *Clouds and Climate* (Gidrometeoizdat, Leningrad, 1986), 512 pp.
7. G.E. Landsberg, *Climate of a City* (Gidrometeoizdat, Leningrad, 1983), 248 pp.
8. E.L. Kogan, I.P. Mazin, B.N. Sergeev, and V.I. Khvorost'yanov, *Numerical Simulation of Clouds* (Gidrometeoizdat, Moscow, 1984), 185 pp.
9. V.B. Nesterenko, A.A. Mikhalevich, and B.E. Tverkhovskin, *Fast Reactors and Heat−Exchange Devices of Nuclear Plants with a Dissociating Heat−Transfer Agent* (Minsk, 1978).
10. E.N. Teverovskii, ed., *Permissible Emissions of Radioactive and Chemical Substances into the Atmosphere* (Energoatomizdat, Moscow, 1985).
11. E.P. Vishnevskii, S.I. Zanov, and V.G. Pimkin, Izv. Akad. Nauk Bellorussk. SSR, Ser. Fiz.−Energeticheskikh Nauk, No. 1, 9−15 (1989).